

# Developing Capability for Hydride Moderator Manufacturing to Facilitate Thermal Spectrum Design Options



Xunxiang Hu  
Chinthaka Silva  
Kurt A. Terrani

**September 27, 2019**

M2CT-19OR06090122

## DOCUMENT AVAILABILITY

Reports produced after January 1, 1996, are generally available free via US Department of Energy (DOE) SciTech Connect.

**Website** [www.osti.gov](http://www.osti.gov)

Reports produced before January 1, 1996, may be purchased by members of the public from the following source:

National Technical Information Service  
5285 Port Royal Road  
Springfield, VA 22161  
**Telephone** 703-605-6000 (1-800-553-6847)  
**TDD** 703-487-4639  
**Fax** 703-605-6900  
**E-mail** [info@ntis.gov](mailto:info@ntis.gov)  
**Website** <http://classic.ntis.gov/>

Reports are available to DOE employees, DOE contractors, Energy Technology Data Exchange representatives, and International Nuclear Information System representatives from the following source:

Office of Scientific and Technical Information  
PO Box 62  
Oak Ridge, TN 37831  
**Telephone** 865-576-8401  
**Fax** 865-576-5728  
**E-mail** [reports@osti.gov](mailto:reports@osti.gov)  
**Website** <http://www.osti.gov/contact.html>

This report was prepared as an account of work sponsored by an agency of the United States Government. Neither the United States Government nor any agency thereof, nor any of their employees, makes any warranty, express or implied, or assumes any legal liability or responsibility for the accuracy, completeness, or usefulness of any information, apparatus, product, or process disclosed, or represents that its use would not infringe privately owned rights. Reference herein to any specific commercial product, process, or service by trade name, trademark, manufacturer, or otherwise, does not necessarily constitute or imply its endorsement, recommendation, or favoring by the United States Government or any agency thereof. The views and opinions of authors expressed herein do not necessarily state or reflect those of the United States Government or any agency thereof.

Transformational Challenge Reactor

**DEVELOPING CAPABILITY FOR HYDRIDE MODERATOR MANUFACTURING TO  
FACILITATE THERMAL SPECTRUM DESIGN OPTIONS**

Xunxiang Hu  
Chinthaka Silva  
Kurt A. Terrani

Date Published: September 27, 2019

M2CT-19OR06090122

Prepared by  
OAK RIDGE NATIONAL LABORATORY  
Oak Ridge, TN 37831-6283  
managed by  
UT-BATTELLE, LLC  
for the  
US DEPARTMENT OF ENERGY  
under contract DE-AC05-00OR22725



# CONTENTS

CONTENTS.....	i
LIST OF FIGURES.....	ii
LIST OF TABLES.....	iii
ACRONYMS.....	iv
ACKNOWLEDGMENTS.....	v
ABSTRACT.....	vi
1. INTRODUCTION.....	1
2. OVERVIEW OF YTTRIUM HYDRIDE.....	2
2.1 Thermodynamics of the Y-H binary system.....	2
2.2 Bulk Properties of YH <sub>x</sub> .....	5
3. FABRICATION AND CHARACTERIZATION OF YTTRIUM HYDRIDE.....	6
3.1 Hydriding process.....	6
3.2 Crack-free Yttrium Hydrides.....	8
4. DESIGN OF A NEW HYDRIDING SYSTEM.....	11
5. SUMMARY.....	13
6. REFERENCES.....	13

## LIST OF FIGURES

Figure 1. Phase diagram of Y-H system [19].....	3
Figure 2. Experimental isotherms for the Y-H and Y-D systems [13]. .....	4
Figure 3. Equilibrium hydrogen partial pressures of $ZrH_{1.7}$ and $YH_{1.7}$ as a function of temperature. ....	5
Figure 4. Thermal conductivity of $\delta$ - $YH_x$ and $\delta$ - $ZrH_x$ . .....	6
Figure 5. Schematic plot of the static hydriding system. ....	7
Figure 6. As-fabricated yttrium hydride disks, rods, and hexagonal coupons.....	9
Figure 7. XCT images of $YH_x$ pellets (a. YHR-1 and b. YHR-2) and the snapshots of cross sections.....	10
Figure 8. XRD pattern of $YH_{1.71}$ along with Rietveld refinement fit. ....	11
Figure 9. Schematic plot of the new hydriding system. The picture of Inconel retort is also included. ....	12
Figure 10. The evolution of important parameters during hydriding process. ....	13

## LIST OF TABLES

Table 1. Properties of metal hydrides having potential nuclear application [10] .....	2
Table 2. YHx pellets fabricated by using the static hydriding system.....	8

## ACRONYMS

DOE	US Department of Energy
DSF	Dynamic Structure Factor
FCC	Face Centered Cubic
HCP	Hexagonal Closest Packed
LAMDA	Low Activation Materials Development and Analysis laboratory
ORNL	Oak Ridge National Laboratory
TCR	Transformational Challenge Reactor
XCT	X-ray Computed Tomography
XRD	X-ray Diffraction
YH <sub>x</sub>	Yttrium Hydride
ZrH <sub>x</sub>	Zirconium Hydride



## **ACKNOWLEDGMENTS**

This work was supported by the US Department of Energy, Office of Nuclear Energy (DOE-NE). The authors thank A.R. Marquez for his assistance in performing XCT measurement. The report was authored by UT-Battelle under contract No. DE-AC05-00OR22725 with the DOE.

## ABSTRACT

This report provides a summary of efforts to develop the capability to fabricate massive crack-free yttrium hydride samples to support thermal spectrum design options for the Transformational Challenge Reactor (TCR) in FY2019. The challenges to fabricating massive, crack-free single-phase yttrium hydride are discussed. By using a modified static hydriding system, we have successfully demonstrated the fabrication of crack-free yttrium hydride, guided by the well-established thermodynamics of the binary yttrium-hydrogen system. The presence of  $\alpha$ -phase yttrium in the fabricated yttrium hydride necessitates employing temperature-pressure isochore cooling at the end of the hydriding process. Thus, a fully programmable hydriding system with continuous hydrogen partial pressure and flow control coordinated with precise temperature control has been designed to facilitate processing of massive, crack-free metal hydrides with the desired H/Y atom ratio. The new system is capable of fabricating yttrium hydride samples that will be used to establish a complete database of yttrium hydride to support the application of yttrium hydride as a high-performance moderator material in the TCR and other nuclear systems.

## 1. INTRODUCTION

Hydrogen has broad applications in both nuclear and non-nuclear systems [1]. Hydrogen is an outstanding moderator for neutrons of less than a few MeV of kinetic energies in nuclear systems by reason of its substantial equivalence in mass to the neutron, its low neutron absorption cross section, and its acceptably high neutron scattering cross section. This characteristic is useful for slowing down fission neutrons to a level at which they have a greater probability of interacting with other fissile, fertile, and neutron-control atoms. Given its high energy density, hydrogen itself is also an ideal energy carrier, averts adverse effects on environment, and reduces dependence on imported oil for countries without natural resources. Hydrogen storage is clearly a key enabling technology for the development of a hydrogen economy [2]. Metal hydrides have been perceived as an efficient, low-risk option for high-density hydrogen storage since the late 1970s. Transition metals are known to absorb large quantities of hydrogen to form metal-hydrogen solid solution at low hydrogen content and the hydride compounds at higher hydrogen content. The atomic density of hydrogen in many of these materials is far greater than in liquid hydrogen itself.

Metal hydrides are particularly well suited to thermal reactor system in which core weight and volume need to be minimized, where they serve as a constituent in fuels and in moderator and shield materials. Table 1 shows the basic properties of selected metal hydrides that have potential application in nuclear systems. It is apparent that zirconium hydride ( $ZrH_x$ ) and yttrium hydride ( $YH_x$ ) are two most promising moderator materials in terms of the moderating ratio (the ratio of the macroscopic slowing-down power to the macroscopic cross section for neutron absorption). Actually,  $ZrH_x$  has been frequently used as a high-performance moderating material in advanced reactors. Examples include the Systems Nuclear Auxiliary Power (SNAP) Program [3]; Training, Research, Isotopes, General Atomic (TRIGA) research reactors [4]; and nuclear thermal propulsion reactors [5]. In these cases,  $ZrH_x$  is purposefully used as the matrix for fissile materials in nuclear fuel applications. The most common type of hydride fuel consists of metallic uranium dispersed in a  $ZrH_x$  matrix with a nominal composition of U(30wt%)- $ZrH_{1.6}$ . Higher power density, high moderator density inherent to the fuel, large prompt negative fuel-temperature reactivity feedback, and higher thermal conductivity are attractive attributes of this class of fuels [4].

Large, hexagonal-cross-section rods of clad  $YH_x$  each with a central axial hole for a fuel element and coolant channel were moderator elements in the gas-cooled Aircraft Nuclear Propulsion reactor developed by General Electric. It was easily capable of operating at 1200°C at some sacrifice of hydrogen concentration [6, 7]. Following several decades of hiatus in constructing advanced reactors, U.S. DOE recently launched a plan to build and operate an additively manufactured microreactor at Oak Ridge National Laboratory (ORNL), the Transformational Challenge Reactor (TCR), to demonstrate a faster, more affordable approach to advanced nuclear energy [8].  $YH_x$  was selected as the leading moderator material for this reactor. In addition to its outstanding neutron moderating characteristics, hydrogen (particularly as a metal hydride) offers other unique nuclear advantages when it is used as a shield component, e.g., because of its high electron-to-mass ratio, hydrogen is the best Compton-effect scatterer and energy degrader for gamma- and X-rays. However, the cost limits its application as a radiation shield. Yttrium hydride was also proposed for use in reactivity control elements for fast-spectrum nuclear reactors; the temperature variation of the hydride would provide attendant reversible changes in the equilibrium concentration of hydrogen, which in turn would control the reactivity [9]. The lack of available high-purity yttrium metal and its cost (30 times the cost of metal zirconium[10]) limited the application of yttrium hydride in nuclear systems in the early era of nuclear energy. The reduced price of ultra-high purity yttrium metal (99.99%, ~\$1400/kg) in the new century makes the broad nuclear application for  $YH_x$  more likely.

**Table 1. Properties of metal hydrides having potential nuclear application [10]**

Hydride	Attainable hydrogen density		Hydride density (g/cm <sup>3</sup> )	Slowing down power	Moderating ratio
	10 <sup>22</sup> atoms H/cm <sup>3</sup>	g H/cm <sup>3</sup>			
TiH <sub>2</sub>	9.1	0.152	3.78	1.85	6.3
ZrH <sub>2</sub>	7.3	0.122	5.56	1.45	55
LiH	5.8	0.095	0.78	1.2	3.5
YH <sub>2</sub>	5.8	0.097	4.24	1.2	25
ThH <sub>2</sub>	4.9	0.082	9.5	1.0	5.2
H <sub>2</sub> O	6.6	0.110	0.98	1.35	70
ThZr <sub>2</sub> H <sub>7</sub>	7.7	0.129	7.75	1.55	14
ThTi <sub>2</sub> H <sub>6</sub>	8.8	0.147	8.15	1.8	6

There is a need for thermally and chemically stable massive metal hydrides for use in shield, reflector, moderator, and moderator-fuel in nuclear reactor components. The common method of preparing metal hydrides is by direct reaction of the metal with hydrogen, guided by the phase diagram and the pressure-composition-temperature relationship. The reaction of hydrogen with the metals (e.g. Zr, Y, Ti, Th) is a diffusion-controlled exothermic process that normally results in expansion of the metal lattice as the hydrogen enters portions of the lattice. This gives rise to a substantial decrease in density and represents a significant volume expansion during the hydriding process (e.g., 19% in the case of TiH<sub>2</sub>, 17% in the case of ZrH<sub>2</sub>, 6% in the case of YH<sub>2</sub>). Such changes produce severe stresses in the massive metal hydrides since the diffusive nature of the hydriding process results in a large hydrogen concentration gradient. During the hydriding process, a hydride case forms on the surface and hydrogen is in solid solution in the interior of the specimen. At the interface between the hydride case and the interior, the growth accompanying hydride formation generates stresses that can easily exceed the fracture strength of the hydride and cause extensive cracking. Therefore, to prepare massive single-piece forms of metal hydride forms, this cracking must be avoided—which is challenging [11] [12].

In this report, we summarize our efforts to develop the capability to fabricate massive crack-free yttrium hydride for its application as a high performance moderator material in the TCR and other advanced nuclear reactors.

## 2. OVERVIEW OF YTTRIUM HYDRIDE

### 2.1 THERMODYNAMICS OF THE Y-H BINARY SYSTEM

The yttrium-hydrogen (Y-H) binary phase diagram and the pressure-composition-temperature relationship are the two most important pieces of information needed to guide the fabrication of yttrium hydride. A reliable binary Y-H phase diagram was established in the late 1970s at ORNL after the availability of ultra-high-purity yttrium metal [13]. Figure 1 shows the phase diagram for Y-H system. The yttrium hydrogen solid solution ( $\alpha$  phase), the di-hydride ( $\delta$  phase), and the tri-hydride ( $\epsilon$  phase) are present. In the  $\alpha$ -phase region, the hydrogen atoms reside in the lower energy tetrahedral interstitial sites of the hexagonal closest packed (HCP) yttrium lattice ( $a=0.36474\text{nm}$ ,  $c=0.57306\text{nm}$ ). The di-hydride ( $\delta$  phase) has a face-centered cubic (FCC) crystal structure ( $a=0.5207\text{nm}$ ) with a CaF<sub>2</sub> prototype structure (space group: Fm-3m) in which yttrium atoms occupy the face centers and corners of the unit cell and hydrogen atoms occupy the tetrahedral and octahedral interstitial sites within the lattice. Hydrogen atoms prefer to occupy the lower-

energy tetrahedral locations; and it was initially believed that in the dihydride configuration, all H atoms would be in the tetrahedral sites [14] which, when fully loaded would yield  $Y_4H_8$ , i.e.,  $YH_2$ . However, it was later shown that octahedral sites are partially occupied before the tetrahedral sites are completely filled at  $x < 2$  [15-17]. The site occupancy is also temperature dependent. Khatamian et al. [18], working with  $YH_{1.98}$  at 11K and 300K, observed a lower H octahedral site occupancy at 11K compared with 300 K and suggested this to be related to the migration of hydrogen atoms to higher-energy octahedral sites with thermal activation. On the other hand, Goldstone et al. [16] studied the site occupancy of  $YH_{2.0}$  between 15 and 420 K and demonstrated octahedral occupancy, which tended to decrease with increasing temperature, contrary to what was expected. Additional work is needed to confirm the hydrogen position in  $\delta$ - $YH_x$ . In the  $\epsilon$  phase region, hydrogen atoms occupy all available interstitial sites in the HCP structure of  $YH_3$  ( $a=0.63587\text{nm}$ ,  $c=0.66068\text{nm}$ ).

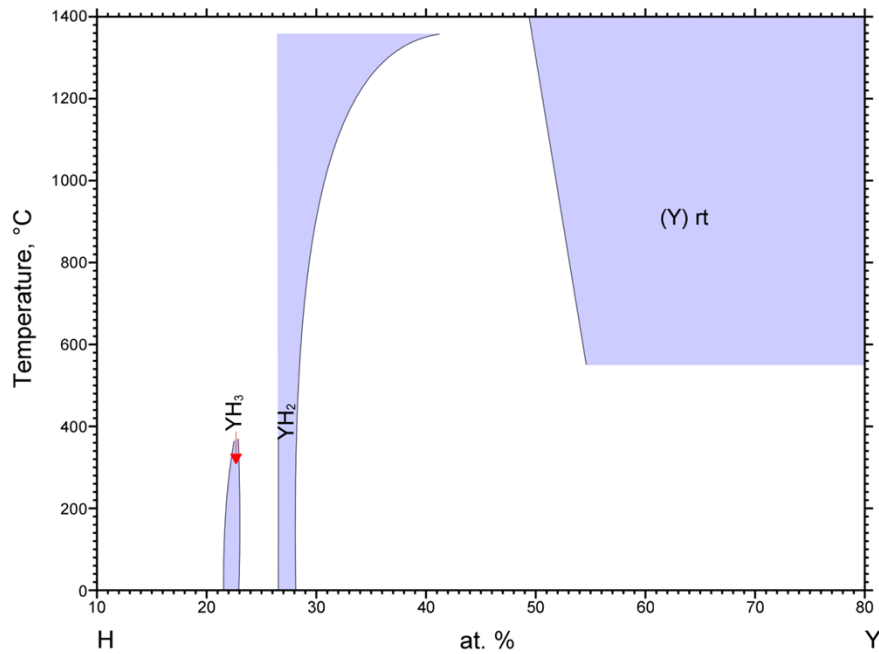


**Figure 1. Phase diagram of Y-H system [19].**

Begun et al.[13] reported the equilibrium hydrogen pressures as a function of the H/Y atom ratio and temperature of Y-H isotope system. Fu et al. [20] performed a coupled experimental and thermodynamic modeling study of the Y-H system and reported the similar results to Begun's work. The experimental isotherms for the Y-H and Y-D systems were shown in Figure 2. In the low composition range, the logarithm of the equilibrium hydrogen pressure increases linearly with the logarithm of the H/Y atom ratio. In this region, only the solid phase exists, an interstitial solid solution of atomic hydrogen in metal Y. Then as the concentration of dissolved hydrogen is increased the equilibrium hydrogen pressure reaches a plateau and the curve becomes relatively flat. In this region two condensed phases exist in equilibrium: the solid solution of atomic hydrogen in metal yttrium, and a hydrogen-deficient  $YH_2$  phase. With the addition of more hydrogen and a corresponding increase in the H/Y atom ratio, the curve starts to slope upward indicating a single-phase region once again, i.e., the slightly hydrogen-deficient  $YH_2$  phase [13, 20].

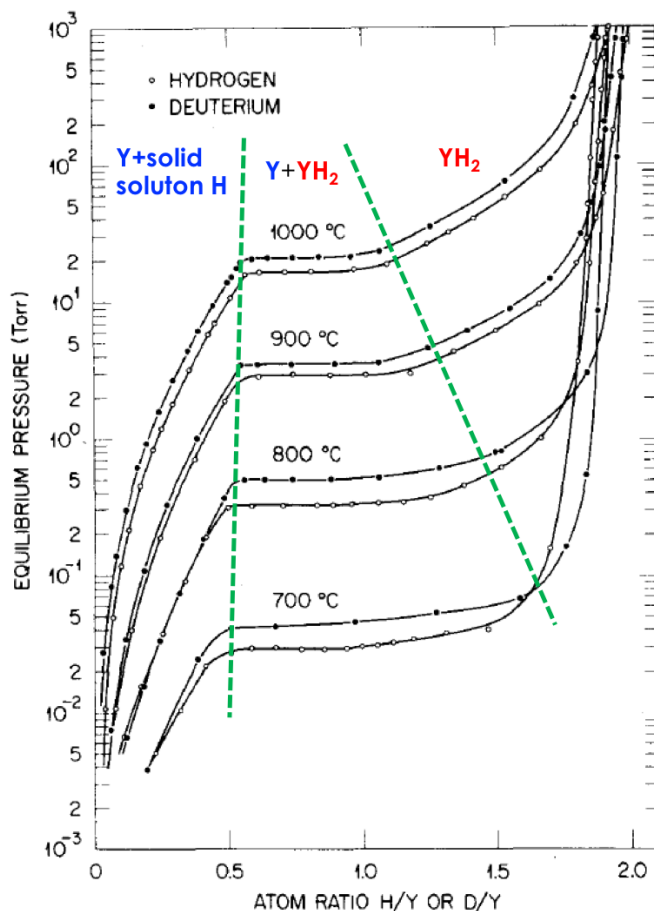


**Figure 2. Experimental isotherms for the Y-H and Y-D systems [13].**

Yttrium hydride offers unique advantages as a moderator for high-temperature thermal nuclear reactors. In contrast to other hydrides under consideration as moderator, this material retains its relatively high content of hydrogen at elevated temperatures. As shown in Figure 2, the equilibrium hydrogen pressure of  $\delta$  phase  $YH_x$  at 1000°C is always less than 1 atm. Figure 3 exhibits a direct comparison of the equilibrium hydrogen partial pressures of  $ZrH_{1.7}$  and  $YH_{1.7}$  as a function of temperature. The hydrogen pressure required to maintain the thermodynamic equilibrium of  $YH_{1.7}$  is 2.5~4.5 orders of magnitude lower than that of  $ZrH_{1.7}$  at the same temperatures, indicating that  $YH_x$  has superior thermal stability over  $ZrH_x$ . The application of  $ZrH_x$  in nuclear systems required careful management of the moderator temperature and additional effort to develop a hydrogen barrier to mitigate hydrogen desorption at elevated temperatures [7]. In contrast, the thermodynamic driving force for H desorption from  $YH_x$  is significantly smaller and results in its stability at elevated temperatures.

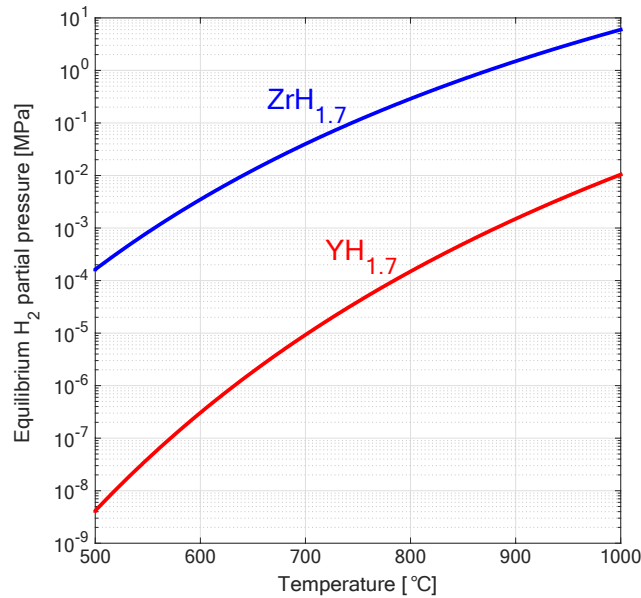


**Figure 3. Equilibrium hydrogen partial pressures of  $ZrH_{1.7}$  and  $YH_{1.7}$  as a function of temperature.**

## 2.2 BULK PROPERTIES OF YHX

The basic bulk properties of single-phase  $YH_x$  have not been extensively studied because of the challenge of fabricating single-phase  $\delta$ - $YH_x$ , although such data are much needed for practical use. To facilitate the fabrication of bulk single-phase  $YH_x$  and to improve the understanding of the stability of  $YH_x$ , the kinetics of hydrogen absorption on and desorption from  $YH_x$  and metal Y as well as H diffusion rates in these phases needs to be investigated. While this information was codified previously by the authors for the  $ZrH_x$  system [21] [22], it is currently unavailable for the  $YH_x$  system and will be tackled in the near future under the TCR program. A Japanese research group reported the physical, thermal, and mechanical properties of single phase  $YH_x$  through a systematic study [23-25]. Based on the available data, the thermal conductivity of  $YH_x$ —one of the critical properties for its moderator application in nuclear reactors—does not show a significant hydrogen concentration dependence but has a strong temperature dependence, as shown in Figure 4. The thermal conductivity of zirconium hydride shows a nearly constant value of 20 W/m/K against temperature [26]. Therefore,  $\delta$ - $YH_x$  is also superior to zirconium hydride when considering heat transport processes in addition to its excellent thermal stability. The elastic moduli and microhardness of  $YH_x$  exhibit a H/Y atom ratio dependence in their studies. However, the hydrogen concentration determination method was not given in these studies, weakening the reliability of the reported results. A robust correlation between the bulk properties of yttrium hydride and the H/Y atom ratio has not been available up to now. In addition, the successful deployment of  $YH_x$  as a high-temperature moderator material in advanced reactors requires a sound understanding of its response to neutron irradiation. However, a database of the physical and thermomechanical properties of neutron-irradiated  $YH_x$  as a function of radiation temperature and radiation dose is not yet available, so a campaign to irradiate  $YH_x$  is in urgent need as well. This area is also being addressed under the TCR program [27] to truly enable adoption of this moderator technology for advanced reactors.

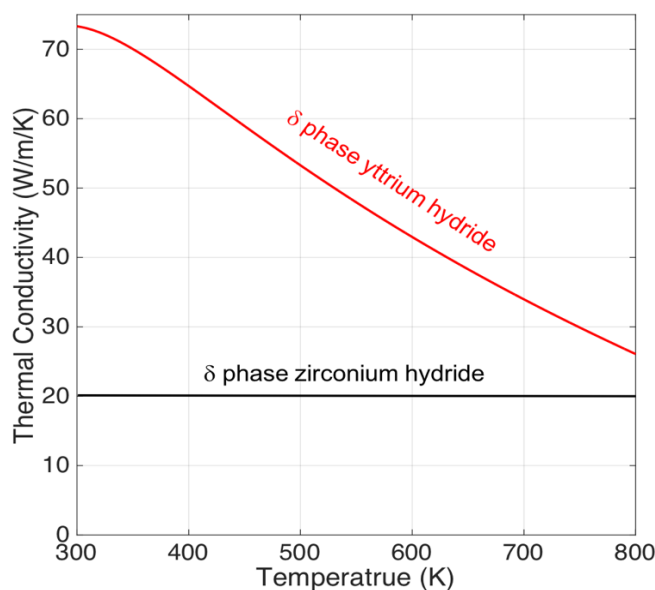


**Figure 4. Thermal conductivity of  $\delta$ -YH<sub>x</sub> and  $\delta$ -ZrH<sub>x</sub>.**

Thermal neutron scattering behavior of YH<sub>x</sub> needs to be thoroughly understood to facilitate the reactor core designs that employ YH<sub>x</sub> as moderator material. Although *Ab initio* approach has been used to predict the neutron scattering cross sections of YH<sub>2</sub> [28], the dependence of the H/Y atom ratio has not been reported. Direct experimental measurement of the neutron scattering cross section also has not been carried out. In neutron transport simulation, an approximation is conventionally used in which the total dynamic structure factor (DSF) of YH<sub>2</sub> is first artificially separated into the two components—one corresponding to yttrium in YH<sub>2</sub> and the one to hydrogen—that make up the total DSF. Then for values of H/Y < 2.0, the DSF is approximated as a weighted sum of those two components, where the weights reflect the modified atom ratio of yttrium and hydrogen in YH<sub>x<2.0</sub>. The accuracy of this approximation is unknown. More systematic study on the neutronic property of YH<sub>x</sub> is needed and will be undertaken under the TCR program.

Therefore, it is the objective of the TCR program to establish a complete database of YH<sub>x</sub> bulk properties to facilitate the reactor designs that employ YH<sub>x</sub>. The first step was to set up a routine to fabricate single phase YH<sub>x</sub>, which is the emphasis of this report.

### 3. FABRICATION AND CHARACTERIZATION OF YTTRIUM HYDRIDE

#### 3.1 HYDRIDING PROCESS

As stated in the Introduction, fabrication of metal hydrides is achieved through the direct reaction of metals and hydrogen at high temperature. Yttrium hydrides with desired H/Y atom ratios may be fabricated in a variety of ways, e.g., by introducing measured amount of hydrogen into small-volume retorts or by carefully matching retort temperature and hydrogen pressure. In the current work, the first method was employed. Yttrium hydride may also be fabricated via the powder sintering route as demonstrated by researchers at Los Alamos National Laboratory [29]. However, the sintering process is cumbersome, allows for far simpler geometries than what is viable by bulk metal hydriding, and is likely to result in introduction of impurities in the hydride. Given these issues and no obvious benefit, the sintering route for yttrium hydride processing will not be pursued under the TCR program.



A hydriding system (Figure 5) with an ultra-high vacuum level of  $1 \times 10^{-7}$  torr was established by modifying the permeation testing station [30] located at the ORNL Low Activation Materials Development and Analysis (LAMDA) lab for the fabrication of yttrium hydride. The maximum temperature of the furnace in this system is  $1100^\circ\text{C}$ . A quartz retort was used to minimize the permeation of hydrogen at elevated temperatures.

The most significant challenge in fabricating massive crack-free bulk metal hydride is that the hydrogen concentration gradient across the sample body resulting in differential strain and stress, and ultimately may result in cracking. The prevention of cracking then would appear to be clearly a matter of preventing large concentration gradients within the sample. Therefore, hydriding was initiated at the desired final equilibration temperature; but the rate of hydriding at said temperature was limited to allow more time for hydrogen redistribution (via bulk diffusion process) within the workpiece and thus avoid an adverse hydrogen concentration gradient in the sample. Uniformity of retort temperature is generally of primary importance in producing sound massive metal hydrides with uniform hydrogen/metal atom ratios.

A typical example of the use of the hydriding system is described as follows. A metal yttrium sample is cleaned and wrapped in molybdenum foil and is then inserted to the quartz tube. After the system is evacuated to a vacuum level of  $1 \times 10^{-7}$  torr, the metal yttrium sample is heated in vacuum to a high temperature for a couple of hours. This high temperature is maintained in the subsequent hydriding process. Then a predetermined amount of hydrogen, corresponding to the wanted H/Y atom ratio of final  $\text{YH}_x$  product, is introduced to the quartz tube at a slow flow rate. Following the consumption of hydrogen, when the equilibrium hydrogen pressure is established in the system, additional annealing time is applied to ensure the homogeneous distribution of hydrogen within the sample. The hydride sample is extracted following a rapid temperature decrease of the system. At the moment, the capability to control the hydrogen partial pressure and temperature during cooling does not exist within this system. The system described in Section 4 will also offer this capability.

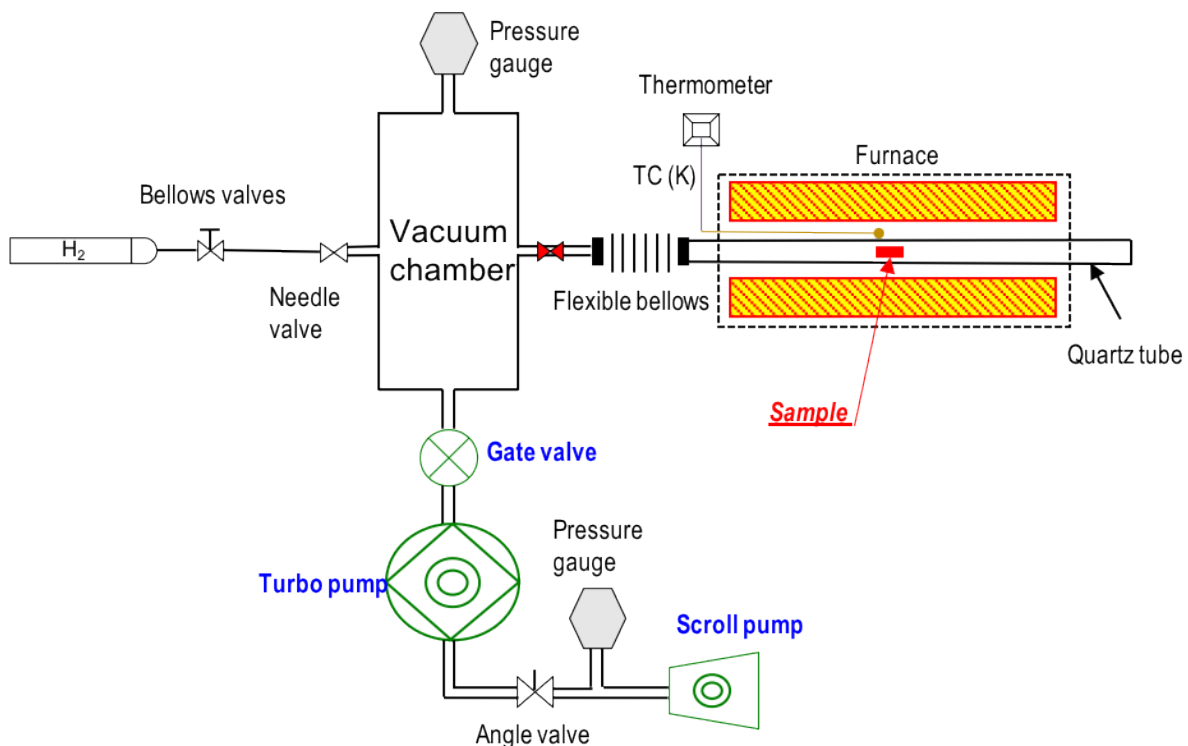


**Figure 5. Schematic plot of the static hydriding system.**

### 3.2 CRACK-FREE YTTRIUM HYDRIDES

Following the above-mentioned fabrication procedure, we have successfully fabricated crack-free  $\text{YH}_x$  disks, pellets, and hexagonal coupons with complicated geometries, as shown in Figure 6. The hydrogen content of the as-fabricated  $\text{YH}_x$  samples was determined based on the weight change, which was assumed to be due to the absorption of hydrogen. Table 2 lists the weight change and the calculated H/Y atom ratio of eight  $\text{YH}_x$  pellets with ~10 mm in diameter and ~10 mm in height. A more accurate hydrogen content determination will be performed by using hot vacuum extraction or inert gas fusion. Note that the H/Y atom ratios of fabricated  $\text{YH}_x$  samples presented in this report were obtained based on the weight change.

**Table 2.  $\text{YH}_x$  pellets fabricated by using the static hydriding system**

<b>Sample</b>	<b>Weight of starting yttrium metal (g)</b>	<b>Weight of as-fabricated <math>\text{YH}_x</math> (g)</b>	<b>Absorbed H amount (mol)</b>	<b>H/Y atom ratio</b>
YHR-1	3.52961	3.59703	0.06742	1.698
YHR-2	3.59013	3.65134	0.06121	1.516
YHR-3	3.98303	4.05440	0.07137	1.593
YHR-4	3.65883	3.73447	0.07564	1.838
YHR-5	3.59282	3.66881	0.07599	1.880
YHR-6	3.49813	3.56571	0.06758	1.716
YHR-7	3.74670	3.81094	0.06424	1.524
YHR-8	3.62408	3.69860	0.07452	1.828

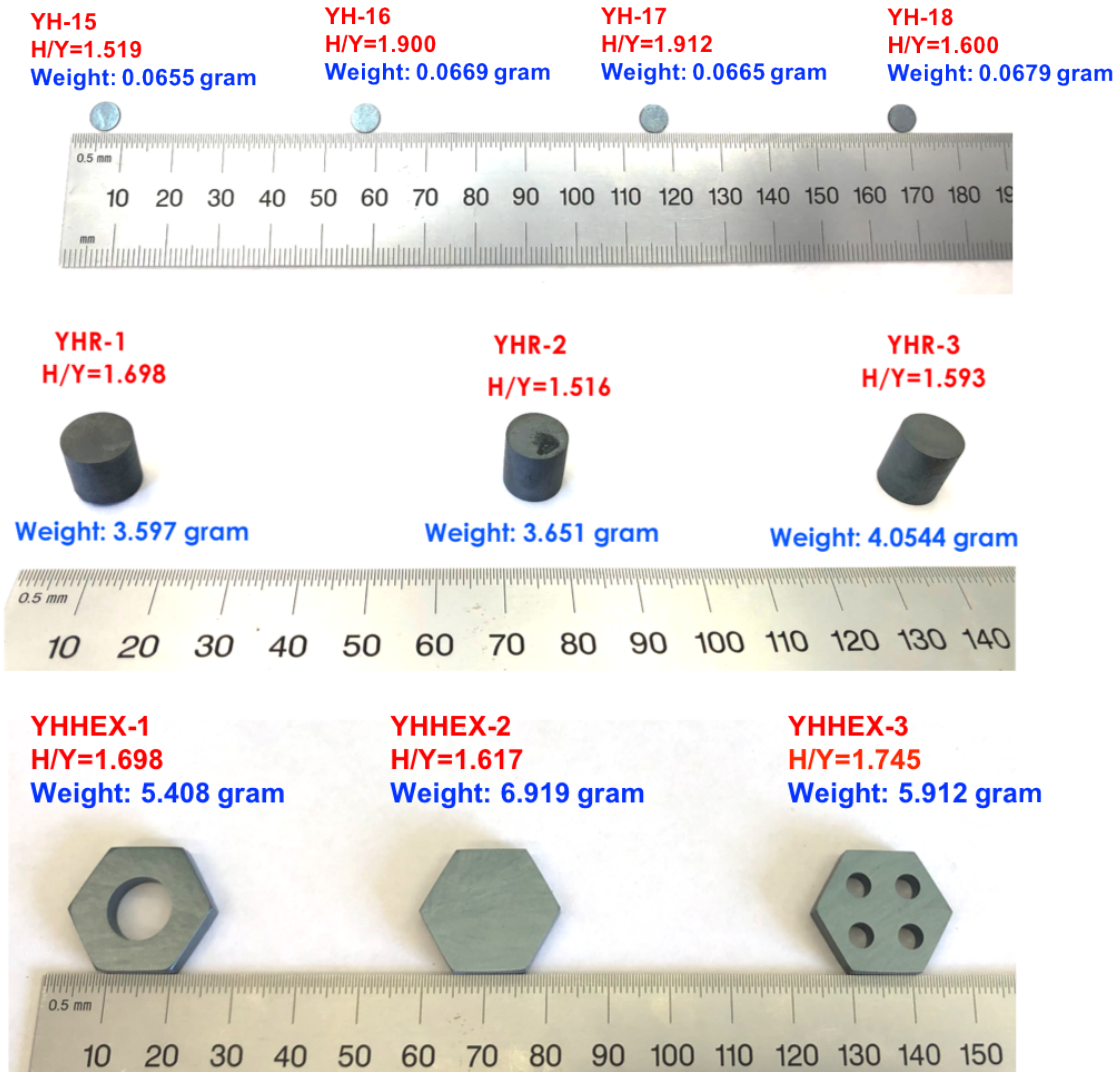


**Figure 6. As-fabricated yttrium hydride disks, rods, and hexagonal coupons.**

No surface cracking was observed on the as-fabricated  $\text{YH}_x$  pellets, disks, or hexagonal coupons. X-ray computed tomography (XCT) analysis was used to explore possible internal cracking. XCT measurements were conducted using a ZEISS Metrotom M800 (200 kV/14 W power). A single scan (1 hour) was conducted to evaluate the whole volume of the specimen. The resolution varies from 9~13 voxel size. Figure 7 shows the XCT images of two  $\text{YH}_x$  pellets, i.e., YHR-1 ( $\text{YH}_{1.698}$ ) and YHR-5 ( $\text{YH}_{1.880}$ ), as examples. No cracking was found in any of the tested  $\text{YH}_x$  pellets (YHR-1, YHR-2, YHR-3, YHR-4, and YHR-5).

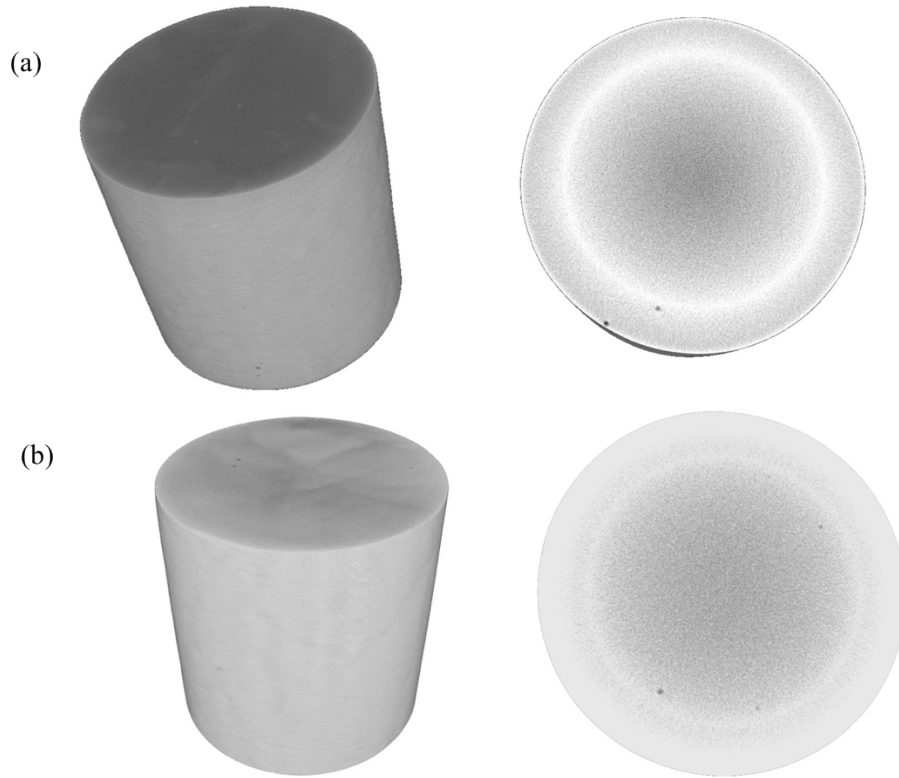


**Figure 7. XCT images of  $\text{YH}_x$  pellets (a. YHR-1 and b. YHR-2) and the snapshots of cross sections**

X-ray diffraction analysis was employed to confirm the phases present in the fabricated hydride samples. XRD samples were prepared by depositing  $\text{YH}_x$  powder on a low-background silicon single-crystal sample holder. Samples were also mixed with lanthanum hexaboride ( $\text{LaB}_6$ ) powder, used as an internal standard during pattern refinement. High-resolution diffraction patterns were obtained using a Bruker D2 Phaser benchtop X-ray diffractometer of 0.30 kW with  $\text{Cu K}\alpha$  radiation. Rietveld refinement was performed on the experimental patterns using General Structure Analysis System [31]. Figure 8 shows an example of the powder XRD pattern of a  $\text{YH}_x$  disk sample ( $\text{YH}_{1.71}$ ). Of the sample, 94.6wt% presented a cubic  $\text{YH}_2$  phase and the rest was  $\alpha$ -yttrium. Note that all fabricated  $\text{YH}_x$  samples exhibited two phases following the current hydriding routine. The presence of  $\alpha$ -yttrium can likely be ascribed to the rapid hydrogen desorption on the sample surface at high temperature during the pumping process prior to bringing down the system temperature to room temperature. The absence of any noticeable oxide phase underlines the well-controlled vacuum environment within the system.

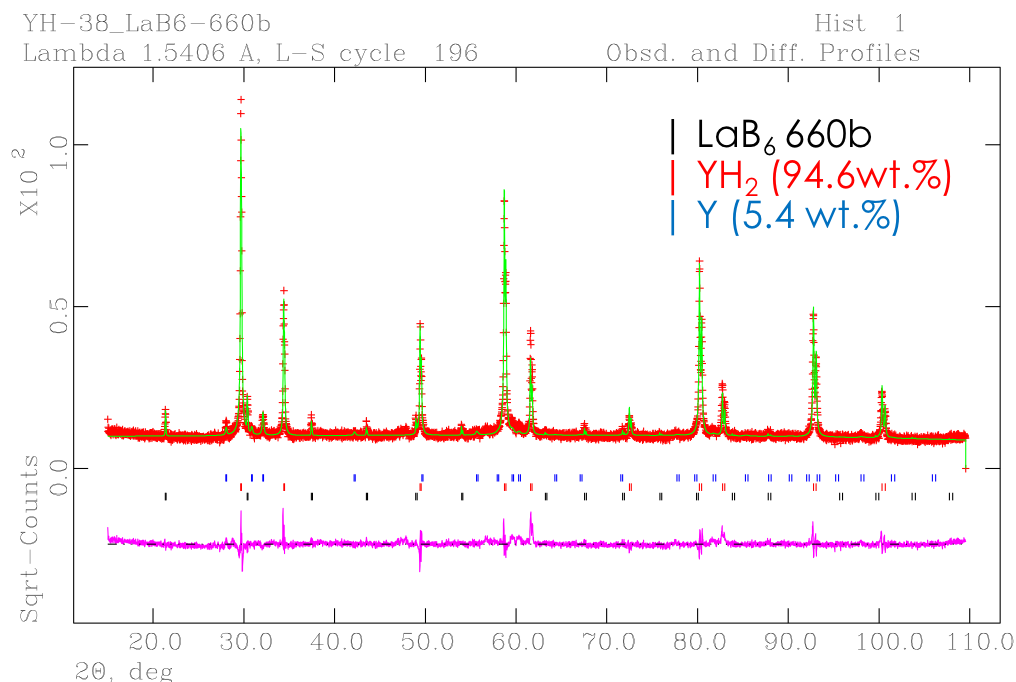


**Figure 8. XRD pattern of YH<sub>1.71</sub> along with Rietveld refinement fit.**

#### 4. DESIGN OF A NEW HYDRIDING SYSTEM

The current hydriding process has demonstrated the successful fabrication of crack-free YH<sub>x</sub> as shown in the previous section. However, due to the lack of simultaneous controls of temperature and hydrogen pressure during the cooling, the H/Y atom ratio of YH<sub>x</sub> at the end of the hydriding process at high temperature cannot be maintained. Therefore, the technique of isochore cooling as a route to maintaining uniform hydrogen distribution in a hydride body need to be applied. An isochore is a line of constant composition on a plot of temperature vs. pressure, which has been well established through thermodynamics studies. Following the isochore line, it is then possible to maintain the initial hydrogen concentration of YH<sub>x</sub> as the elevated temperatures and pressures drop, without either absorbing hydrogen from or evolving it to the surrounding atmosphere. The formed hydride of the desired composition is cooled to room temperature along the isochore line without affecting a change in its composition, particularly without inducing concentration gradients and volume changes at the sample surface [11].

A fully programmable hydriding system with continuous hydrogen partial pressure and flow control coordinated with precise temperature control has been designed and is being constructed to facilitate processing of massive crack-free metal hydrides with desired hydrogen concentration. A schematic plot of this system is shown in Figure 9. It will be an ultra-high vacuum (UHV) system, consisting of all metal parts and fittings, and capable of a vacuum level of  $\sim 1 \times 10^{-7}$  torr at 1000°C. The maximum temperature of the 3-zone tube furnace will be 1100°C. An Inconel retort will be employed to process the sample; it will have an effective working area of 76 mm in diameter and 300 mm in length. A programmable gas control system is designed to enable variable flow control coordinated with temperature control. An automatic emergency cut-off system, including a safety inert gas purge line and pressure relief valve, is being established to ensure safe handling of hydrogen.

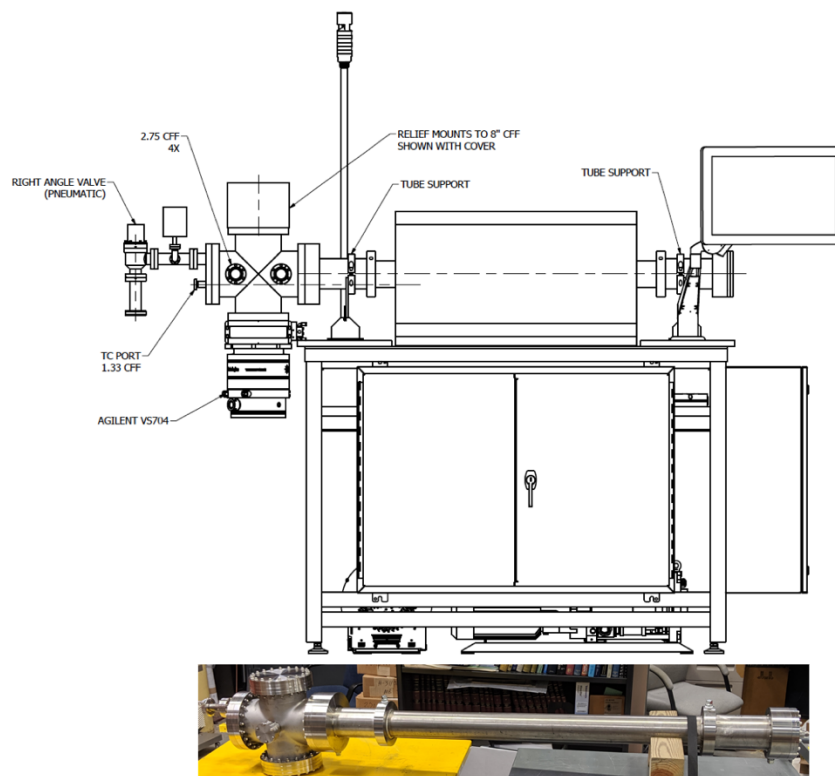


**Figure 9. Schematic plot of the new hydriding system. The picture of Inconel retort is also included.**

The desired hydride will be fabricated by carefully matching the retort temperature and hydrogen pressure. A typical hydriding process is designed as follows: evacuate the retort with samples inside, heat the retort to a high temperature to degas, then lower the retort temperature to the pre-determined processing temperature, isolate the retort from the pumping system, introduce ultra-high-purity hydrogen to the retort at a low flow rate, maintain the hydrogen pressure within the retort to a pre-determined value that together with the processing temperature determines the H/Y atom ratio of the final product, and finally bring the retort to room temperature following the temperature-pressure isochore line. The evolution of the important parameters during the hydriding process is schematically shown in Figure 10. A constant hydrogen flow rate is initially maintained to provide hydrogen supply to the retort. The work piece rapidly absorbs the introduced hydrogen, resulting in a stable vacuum environment in the retort. Then the hydrogen pressure in the retort begins to rise slowly, indicating the onset of the hydrogen saturation of the sample. Eventually, the hydrogen pressure will reach a threshold that is pre-determined based on the desired H/Y atom ratio in the final product and the processing temperature. Then the system pressure will remain constant to enable homogeneous distribution of the hydrogen across the sample. During the cooling down process, the temperature-pressure isochore line is followed to maintain the H/Y atom ratio in the final product.

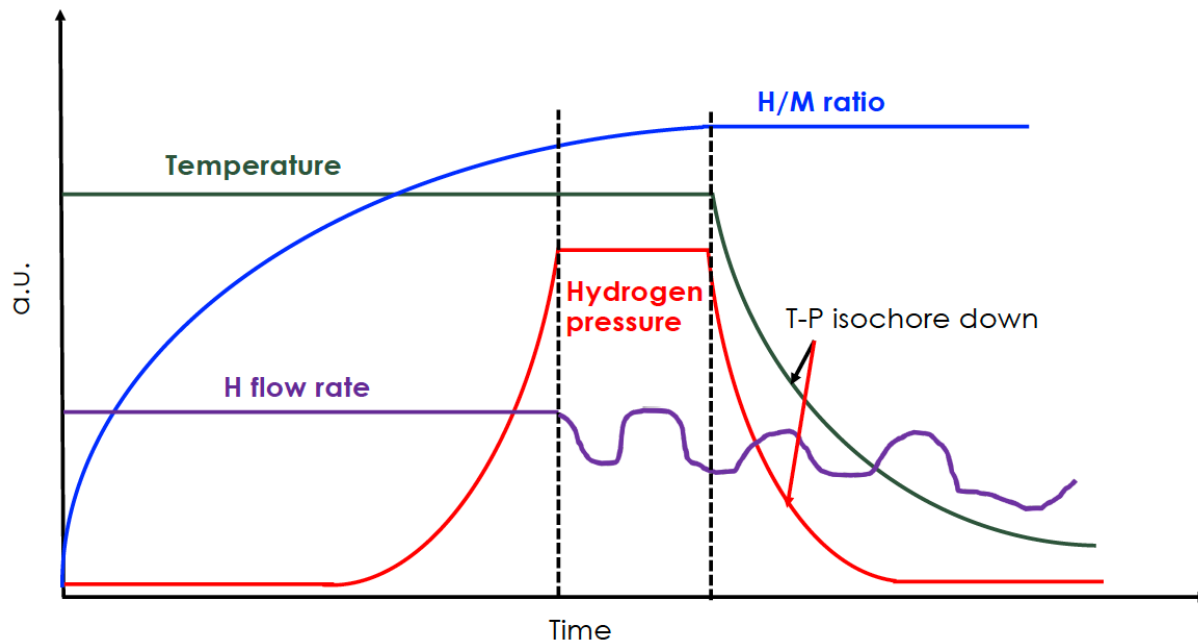


Figure 10. The evolution of important parameters during hydriding process.

## 5. SUMMARY

In this report, we briefly summarize the thermodynamics of the binary Y-H system and the available bulk properties of  $\delta$  phase yttrium hydride. The challenges in fabricating massive crack-free single-phase yttrium hydride are discussed. Using a modified static hydriding system, we have successfully demonstrated the fabrication of crack-free yttrium hydride. A fully programmable hydriding system with continuous hydrogen partial pressure and flow control, coordinated with precise temperature control, has been designed to facilitate the processing of massive, crack-free metal hydrides with the desired H/Y atom ratio. Work is under way to construct the new system to fabricate yttrium hydride samples for the establishment of a complete database of yttrium hydride. The database will be used to support the application of yttrium hydride as a high-performance moderator material in nuclear systems.

## 6. REFERENCES

1. Edwards, P.P., V.L. Kuznetsov, and W.I. David, *Hydrogen energy*. Philos Trans A Math Phys Eng Sci, 2007. **365**(1853): p. 1043-56.
2. Sakintuna, B., F. Lamaridarkrim, and M. Hirscher, *Metal hydride materials for solid hydrogen storage: A review*. International Journal of Hydrogen Energy, 2007. **32**(9): p. 1121-1140.
3. Davies, N. and R. Forrester, *Effects of irradiation on hydrided zirconium-uranium alloy NAA 120-4 experiment*. 1970, Atomics International Div.: Canoga Park, CA.
4. Simnad, M., *The U-ZrHx alloy: Its properties and use in TRIGA fuel*. Nuclear Engineering and Design, 1981. **64**(3): p. 403-422.
5. Haslett, R., *Space Nuclear Thermal Propulsion Program*. 1995, Grumman Aerospace Corp.: Bethpage, NY.

6. Miller, A.J., *Aircraft Nuclear Propulsion Project Semiannual Progress Report*. ORNL-2599, 1959.
7. Vetrano, J.B., *Hydrides as neutron moderator and reflector materials*. Nuclear Engineering and Design, 1971. **14**(3): p. 390-412.
8. <https://tcr.ornl.gov>.
9. Anderson, J.L., W. Mayo, and E. Lantz, *Reactivity control of fast-spectrum reactors by reversible hydriding of yttrium zones*. 1968. **NASA TN D-4615**.
10. Van Houten, R., *Selected Engineering And Fabrication Aspects Of Nuclear Metal Hydrides (Li, Ti, Zr, And Y)*. Nuclear Engineering and Design, 1974. **31**: p. 434-448.
11. Van Houten, R., *Massive Metal Hydride Structures And Methods For Their Preparation*. US3720752, 1973.
12. Van Houten, R., *Hydriding Process*. US3720751, 1973.
13. Begun, G.M., J.F. Land, and J.T. Bell, *High temperature equilibrium measurements of the yttrium-hydrogen isotope (H<sub>2</sub>, D<sub>2</sub>, T<sub>2</sub>) systems*. The Journal of Chemical Physics, 1980. **72**(5): p. 2959-2966.
14. Flotow, H.E., D.W. Osborne, and K. Otto, *Heat Capacities and Thermodynamic Functions of YH<sub>2</sub> and YD<sub>2</sub> from 5° to 350° K and the Hydrogen Vibration Frequencies*. The Journal of Chemical Physics, 1962. **36**(4): p. 866-872.
15. Weaver, J., R. Rosei, and D. Peterson, *Electronic structure of metal hydrides. I. Optical studies of Sc H<sub>2</sub>, Y H<sub>2</sub>, and Lu H<sub>2</sub>*. Physical Review B, 1979. **19**(10): p. 4855.
16. Goldstone, J., et al., *Temperature dependence of hydrogen site occupancy in Yttrium dihydride*. Solid state communications, 1984. **49**(5): p. 475-478.
17. Anderson, D., et al., *Hydrogen locations, diffusion and the electronic density of states in yttrium dihydrides: A nuclear magnetic resonance investigation*. Journal of the Less Common Metals, 1980. **73**(2): p. 243-251.
18. Khatamian, D., et al., *Crystal structure of YD 1.96 and YH 1.98 by neutron diffraction*. Physical Review B, 1980. **21**(6): p. 2622.
19. Khatamian, D. and F.D. Manchester, *H-Y (Hydrogen-Yttrium)*. Binary Alloy Phase Diagram, 1990. **2**: p. 2074-2075.
20. Fu, K., et al., *Experimental investigation and thermodynamic assessment of the yttrium-hydrogen binary system*. Progress in Natural Science: Materials International, 2018. **28**(3): p. 332-336.
21. Terrani, K.A., et al., *The kinetics of hydrogen desorption from and adsorption on zirconium hydride*. Journal of Nuclear Materials, 2010. **397**(1-3): p. 61-68.
22. Hu, X., K.A. Terrani, and B.D. Wirth, *Hydrogen desorption kinetics from zirconium hydride and zirconium metal in vacuum*. Journal of Nuclear Materials, 2014. **448**(1-3): p. 87-95.
23. Ito, M., et al., *Thermal properties of yttrium hydride*. Journal of Nuclear Materials, 2005. **344**(1-3): p. 295-297.
24. Setoyama, D., et al., *Mechanical properties of yttrium hydride*. Journal of Alloys and Compounds, 2005. **394**(1-2): p. 207-210.
25. Ito, M., *Studies on Physical Properties of Metal Hydrides and Hydrogen Behavior in Zr Alloys*. Osaka University, 2008. **PhD Thesis**.
26. Yamanaka, S., et al., *Thermal properties of zirconium hydride*. Journal of Nuclear Materials, 2001. **294**: p. 94-98.



27. P. Champlin, J.B., C. Petrie, X. Hu, K. Linton, R. Howard, K. Terrani, *Capsule and Specimen Geometries for HFIR Irradiation Testing Supporting the Transformational Challenge Reactor*. ORNL/TM-2019/1310, 2019: p. M3CT-19OR06090120
28. Plompen, A., et al., *A thermal neutron scattering law for yttrium hydride*. EPJ Web of Conferences, 2017. **146**.
29. Shivprasad, A.P., et al., *Development of sintered yttrium dihydride compacts for nuclear reactor moderator applications*. Nuclear and Emerging Technology for Space, American Nuclear Society Topical Meeting, 2019.
30. Hu, X., et al., *Determination of He and D permeability of neutronirradiated SiC tubes to examine the potential for release due to microcracking*. ORNL-TM-2017/362, 2017.
31. Larson, A.C. and R.B. Von Dreele, *General Structure Analysis System* Los Alamos National Laboratory Report LAUR 86-748, 2004.